

Correlation between strain-rate sensitivity and viscous properties derived from dynamic nanoindentation of ultrafine-grained Al–Zn alloys

Nguyen Q. Chinh, Department of Materials Physics, Eötvös Loránd University, H-1117 Budapest, Pázmány Péter sétány 1/A., Hungary
Tamás Csanádi, Institute of Materials Research, Slovak Academy of Sciences, Watsonova 47, 04353 Košice, Slovak Republic
Jenő Gubicza, Department of Materials Physics, Eötvös Loránd University, H-1117 Budapest, Pázmány Péter sétány 1/A., Hungary
Ruslan Z. Valiev, Institute of Physics of Advanced Materials, Ufa State Aviation Technical University, 12 K. Marx str., Ufa 450000, Russia; Laboratory for Mechanics of Bulk Nanostructured Materials, Saint Petersburg State University, 28 Universitetsky pr., Peterhof, Saint Petersburg, 198504, Russia

Address all correspondence to Nguyen Q. Chinh at chinh@metal.elte.hu

(Received 8 October 2018; accepted 26 November 2018)

Abstract

The relationship between the oscillatory force and the depth-response during dynamic indentation was analyzed mathematically and investigated experimentally in ultrafine-grained Al–Zn alloys processed by high-pressure torsion. We have shown for the first time that the phase shift between the local oscillatory force and depth signal, caused by the internal friction, is correlated to the strain-rate sensitivity, which is a key parameter indicating the ductility of materials. This correlation enables a new application of dynamic nanoindentation for studying the rate-dependent deformation-mechanisms of materials from a novel aspect.

It is well-established that the application of severe plastic deformation (SPD) techniques, such as high-pressure torsion (HPT), may lead to unique microstructural and mechanical properties of materials exhibiting high strength and enhanced ductility.^[1,2] Recently, ultrafine-grained (UFG) Al–Zn alloys processed by HPT have been extensively studied due to their interesting mechanical behaviors obtained by various compositional designs.^[3–12] For Zn concentrations up to 10 wt%, the hardness of the HPT-processed samples is higher than that of the annealed samples, indicating a normal strengthening effect of SPD.^[7,8,12] In the case of higher Zn concentrations, such as Al–30 wt% Zn alloy, however, there is a strong reduction in hardness due to HPT, showing an abnormal softening effect of SPD.^[12] The abnormal softening was explained by the simultaneous effect of grain refinement and the decomposition of the microstructure during HPT.^[6] It was revealed that the Al/Al grain boundaries of the UFG alloys are wetted by Zn-rich layers that enhance the role of grain boundary sliding, leading to the unusual softening of this UFG material.

The superductility of UFG Al–Zn alloys, which may lead to unusually high elongations of 150%,^[4] is strongly related to their strain-rate sensitivity (SRS) which is a key parameter in the development of superplastic materials. The higher the SRS (conventionally denoted as m) of a material, the more it resists the local reduction of cross-section during tensile tests. Therefore, the measurement of SRS is an important factor in the development of materials with high strength and good ductility. Nanoindentation, which was originally developed for the measurement of hardness and elastic modulus and has become

a widely used technique for mechanical characterization of solids,^[13–23] is an efficient tool also to measure SRS of UFG materials. Despite the numerous works on the determination of SRS by using indentation, its connection with basic viscoelastic properties deriving from dynamic nanoindentation^[24] has not been investigated up to now. Considering the experimental results that the plastic deformation of UFG Al–Zn alloys taking place mainly by grain boundary sliding on Zn-rich wetted layers is an intrinsically viscous process, the objective of the current work is to reveal the correlation between the SRS and the viscoelastic response obtained by dynamic nanoindentation for UFG Al–Zn alloys with wetted grain boundaries.

High purity (4N) Al and Al–Zn alloys with Zn contents of 10 and 30 wt% were prepared by vacuum induction melting. Disks with diameters of 20 mm and thicknesses of 0.8 mm were homogenized at 500 °C for 1 h, then quenched to room temperature and processed by HPT as described in Refs. 6–8. Samples were cut out from the regions at the half-radius of the HPT-processed disks. The microstructure of these specimens consisted of equiaxed ultrafine grains with sizes between 300 and 700 nm.

Dynamic indentation measurements were carried out by using a nanohardness tester NHT-TTX (CSM-Instruments/Anton Paar) device equipped with a Berkovich indenter. The measurements were performed using dynamic nanoindentation mode in load control. This means that the applied load had two components. The main term $F_{lin}(t)$ increased linearly with time (t) up to a maximum load of 50 mN at a loading rate of $v = 0.5 \text{ mN s}^{-1}$. This load was superimposed by an oscillatory

force of $F_{\sin}(t) = F_0 \sin(\omega t)$ with a maximal amplitude of $F_0 = 2$ mN and an angular frequency ω corresponding to the frequency of 2 Hz. The penetration depth (h) caused by the applied load was recorded as a function of time during the measurements which was also a harmonic signal on a semi-static depth function possessing a phase shift compared to the load signal in the form of $h_{\sin}(t) = h_0 \sin(\omega t - \varphi)$. This phase shift (phase difference) caused by the internal friction in a damping medium is essential for the evaluation of the contact stiffness which is necessary for the determination of the hardness and elastic modulus of the sample as a function of the penetration depth.^[24] Here, it is important to note that we analyze only the depth and load signals as a function of time, other properties, like hardness or modulus, are not discussed in the current work.

In order to establish a connection for SRS and viscous properties of UFG Al–Zn alloys, we outline the basic concept of a commonly used viscoelastic models of dynamic nanoindentation.^[24–26] The scheme of this viscoelastic model, as a damped, forced oscillating indenter in contact with a sample, is shown in Fig. 1.

The spring symbolizes the force component raising from the elasticity, while the dashpot describes the damping of the system. The model comprises an effective spring with a stiffness of K_e , an effective dashpot with a damping coefficient of D_e , and a mass of the indenter as m_i .^[24] In the current work, the damping term is important for us as it describes the effect of the rate-dependent behavior of the investigated materials. If this system is excited by a sinusoidal force, $F_{\sin}(t) = F_0 \sin(\omega t)$, the motion equation of the indenter is similar to the well-known classical physical case of the constraint motion for a body, which is moving for a sinusoidal force via spring in a damping media. In order to obtain the harmonic depth response of the oscillating system around an equilibrium position corresponding to a given semi-static load, the following second-order differential equation should be solved^[24]:

$$m_i \frac{d^2 h}{dt^2} + D_e \frac{dh}{dt} + K_e h = F_0 \sin(\omega t). \quad (1)$$

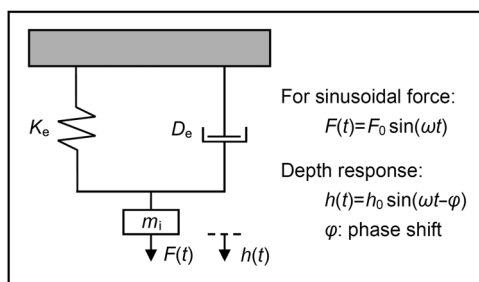


Figure 1. Schematic model describing the collective viscoelastic response of the nanoindenter and the investigated material.

The analytical solution of this equation is also a sinusoidal function with the same ω angular frequency:

$$h(t) = h_{\sin}(t) = h_0 \sin(\omega t - \varphi), \quad (2)$$

where the amplitude:

$$h_0 = \frac{F_0}{\sqrt{(K_e - m_i \omega^2)^2 + (D_e \omega)^2}}, \quad (3)$$

and for the phase shift, φ

$$\tan \varphi = \frac{D_e \omega}{K_e - m_i \omega^2}. \quad (4)$$

In the case of very small phase shift ($\varphi \ll 1$) we can use the usual approximation:

$$\varphi \approx \tan \varphi = \frac{D_e \omega}{K_e - m_i \omega^2}. \quad (5)$$

According to Eqs. (3)–(5), the K_e and D_e values could be evaluated experimentally by measuring the quantities h_0 and φ . Considering the viscoelastic behavior for a given alloy system, for instance, for Al–Zn alloys, where the value of K_e can be expected to be a constant, the phase shift φ given by Eq. (5) is proportional to the value of D_e , indicating that the rate-dependent (or time-dependent) behaviors of materials can be studied by determining the phase shift, φ . This would be the one of the main points of the current work.

As it has been mentioned, during dynamic indentation the applied load is a combination of a linearly increasing component ($F_{\text{lin}}(t) = vt$) and the superimposed sinusoidal signal ($F_{\sin}(t) = F_0 \sin(\omega t)$). Considering the indentation process, the sinusoidal signal can be regarded as the local change of the load on the global component, F_{lin} . For a total load, F_{exp} applied on the indenter:

$$F_{\text{exp}} = F_{\text{lin}} + F_{\sin} = vt + F_0 \sin(\omega t). \quad (6)$$

The corresponding—experimentally measured—total depth-response (h_{exp}) can be given as follows:

$$h_{\text{exp}} = h_{\text{global}} + h_0 \sin(\omega t - \varphi), \quad (7)$$

where the term $h_{\text{global}}(t)$ describes the global development of the depth in the function of time. Selecting a constant depth region, a couple of nanometers in the present case, the global load and depth functions are determined by fitting simple linear functions to F_{exp} and h_{exp} signals. The local force and depth signals are calculated by subtracting the globally fitted lines from the experimental curves. In order to obtain phase shift (φ), both quantities ($F_{\text{exp}} - vt$) and ($h_{\text{exp}} - h_{\text{global}}$) are fitted by the sinusoidal functions $F_0 \sin(\omega t - \varphi_1)$ and $h_0 \sin(\omega t - \varphi_2)$, respectively, in the same time range. Then the phase shift is obtained as a phase difference between the depth and load signals according to $\varphi = \varphi_2 - \varphi_1$.

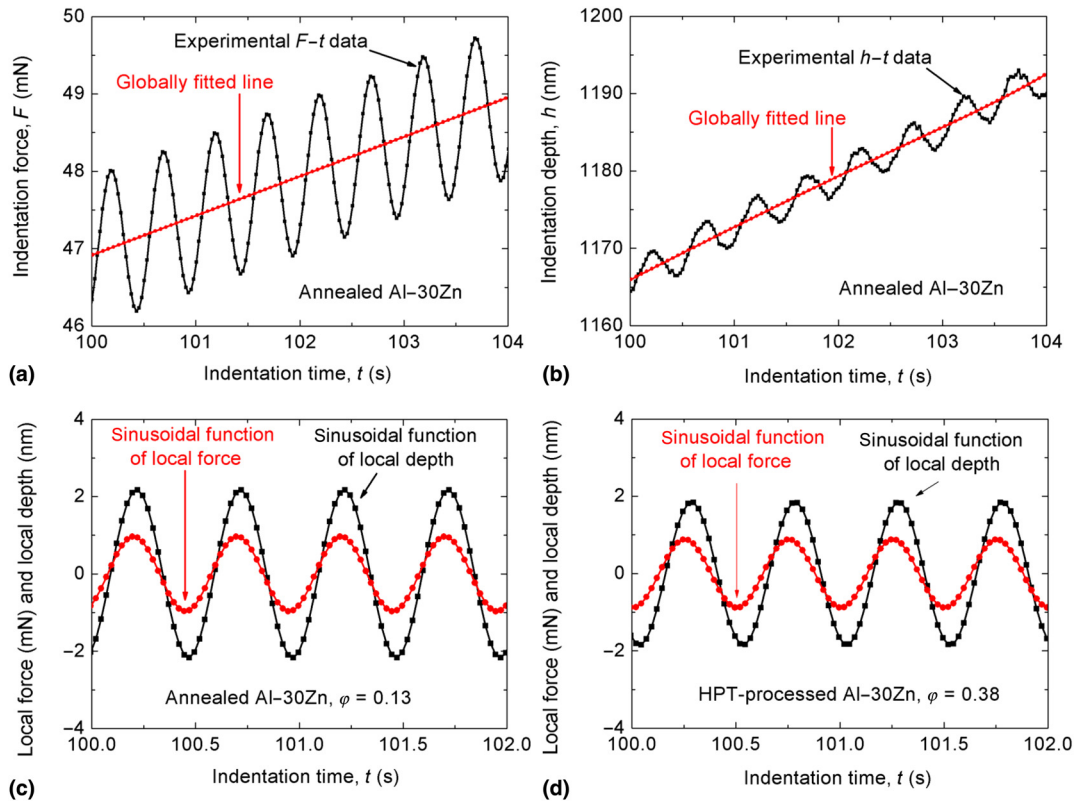


Figure 2. Examples for the main steps of the determination of phase shift (ϕ) during dynamic nanoindentation: (a) and (b) calculation of the local force and depth signals from the experimental curves using globally fitted lines; (c) and (d) the remaining sinusoidal signals by eliminating the global functions for the annealed and HPT-processed Al-30Zn, respectively.

Figure 2 shows some examples demonstrating the determination of ϕ by applying dynamic indentation tests. It should be emphasized that (i) in all experimental cases the local depth-response ($h_0 \sin(\omega t - \phi_2)$) can be fitted well by a sinusoidal function with the same angular frequency than that works for the local force ($F_0 \sin(\omega t - \phi_1)$). Moreover, (ii) as the current work is a pioneer in this subject, the obtained phase shift values could not be compared with the literary data and could not be discussed on that. The ϕ values of 0.13, 0.29, and 0.38 were obtained for annealed Al-30Zn, HPT-processed Al-10Zn, and HPT-processed Al-30Zn samples, respectively, which have the strain rate sensitivity (m) of 0.03,^[27] 0.17, and 0.25,^[12] in the given order.

For the purpose of comparison and explanation, the parameter m is plotted as a function of ϕ in Fig. 3, where the errors of 10% in ϕ and ± 0.02 ^[12] in m are also added. The present experimental results show that there is an unambiguous correlation between the phase shift (ϕ) and the strain rate sensitivity (m). The higher phase shift corresponds to a higher strain rate sensitivity. In the case of the investigated Al-Zn samples, this correlation can be described well by a linear relationship with the function of $m = -0.085 + 0.879\phi$. Although further systematic investigations are needed to clarify the correlation between m and ϕ in details, qualitatively both parameters

express the rate-dependent behavior of the investigated materials.

Considering also the well-established fact that the SRS parameter correlates to the ductility,^[27,28] the preliminary dynamic indentation results may allow us to conclude that the ductility of a material can be studied by investigating its

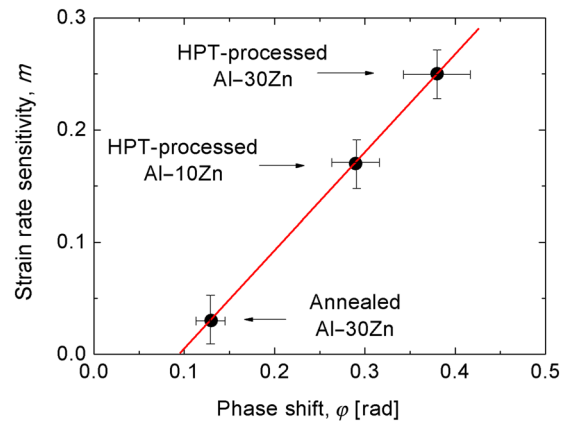


Figure 3. The connection between the obtained phase shift (ϕ) and strain rate sensitivity values (m) of the investigated Al-Zn alloys.

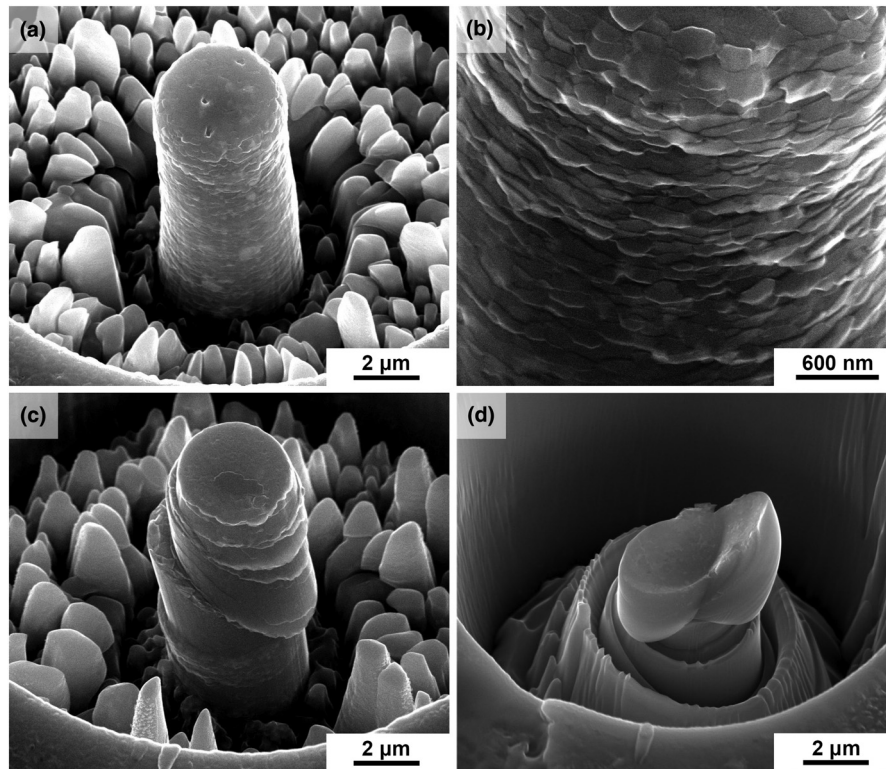


Figure 4. Surface morphologies of compressed micro-pillars for HPT-processed Al–30Zn in low and high magnifications shown in (a) and (b), respectively, (c) HPT-processed Al–10Zn [reproduced with permission from Ref. 12 (Elsevier, 2017)] and (d) annealed Al–30Zn samples [reproduced with permission from Ref. 6 (John Wiley and Sons, 2014)].

phase shift. In the present case, the relatively high phase shift observed in the HPT-processed Al–30Zn sample correlates well to the super-ductility of this sample at room temperature.^[4] The relatively high SRS and phase shift of this sample are certainly a consequence of the high fraction of Al/Al grain boundaries wetted by Zn-rich layers, which lead to intensive grain boundary sliding,^[6,12] as shown in Fig. 4, where the surface morphologies of compressed micro-pillars taken by a scanning electron microscope can be seen.^[6,12] In the case of the HPT-processed Al–30Zn sample [see Figs. 4(a) and 4(b)] the surface morphologies demonstrate clearly the occurrence of intensive grain boundary sliding, as individual ultrafine grains emerging from the pillar surface are visible on the surface.^[12] For the HPT-processed Al–10Zn sample having lower SRS and phase shift (ϕ), only strain localization and individual slip bands are visible [Fig. 4(c)].^[12] The ductility of coarse-grained, annealed Al–30Zn sample having very low SRS and phase shift seems to be very poor,^[6] as only few slip bands are visible in Fig. 4(d).

In summary, a new application of depth-sensing indentation is suggested in the current work. Unique microstructures and mechanical properties of UFG Al–Zn alloys were studied by dynamic nanoindentation testing. We have shown that the phase shift between the oscillatory force and depth-response is well correlated to the strain rate sensitivity, which is a key

parameter in the characterization of the ductility. Our study revealed a possible new application of dynamic nanoindentation in the investigation of rate-dependent deformation-mechanisms in materials.

Acknowledgments

This research was supported by the Hungarian–Russian bilateral Research program (TÉT) No. 2017-2.3.4-TÉT-RU-2017-00005 (NQC and JG). This work was financed partly by the Ministry of Human Capacities of Hungary within the ELTE University Excellence program (1783-3/2018/FEKUTSRAT), by the Ministry of Education and Science of the Russian Federation under grant agreement No. 14.586.21.0061 (unique project identifier RFMEFI58618X0061) (RZV), as well as by the Slovak Grant Agency for Science under the project APVV-15-0469 (TCs).

References

1. A.P. Zhilyaev and T.G. Langdon: Using high-pressure torsion for metal processing: fundamentals and applications. *Prog. Mater. Sci.* **53**, 893 (2008).
2. R.Z. Valiev: Nanostructuring of metals by severe plastic deformation for advanced properties. *Nat. Mater.* **3**, 511 (2004).
3. B.B. Straumal, X. Sauvage, B. Baretzky, A.A. Mazilkin, and R.Z. Valiev: Grain boundary films in Al–Zn alloys after high pressure torsion. *Scripta Mater.* **70**, 59 (2014).

4. R.Z. Valiev, M.Y. Murashkin, A. Kilmametov, B.B. Straumal, N.Q. Chinh, and T.G. Langdon: Unusual super-ductility at room temperature in an ultrafine-grained aluminum alloy. *J. Mater. Sci.* **45**, 4718 (2010).
5. N.Q. Chinh, T. Györi, R.Z. Valiev, P. Szommer, G. Varga, K. Havancsák, and T.G. Langdon: Observations of unique plastic behavior in micro-pillars of an ultrafine-grained alloy. *MRS Commun.* **2**, 75–78 (2012).
6. N.Q. Chinh, R.Z. Valiev, X. Sauvage, G. Varga, K. Havancsák, M. Kawasaki, B.B. Straumal, and T.G. Langdon: Grain boundary phenomena in an ultrafine-grained Al–Zn alloy with improved mechanical behavior for micro-devices. *Adv. Eng. Mater.* **16**, 1000 (2014).
7. E.V. Bobruk, X. Sauvage, N.A. Enikeev, B.B. Straumal, and R.Z. Valiev: Mechanical behavior of ultrafine-grained Al-5Zn, Al-10Zn, Al-30Zn alloys. *Rev. Adv. Mater. Sci.* **43**, 45 (2015).
8. X. Sauvage, M.Y. Murashkin, B.B. Straumal, E.V. Bobruk, and R.Z. Valiev: Ultrafine grained structures resulting from SPD-induced phase transformation in Al–Zn alloys. *Adv. Eng. Mater.* **17**, 1821 (2015).
9. A. Alhamidi, K. Edalati, Z. Horita, S. Hirosawa, K. Matsuda, and D. Terada: Softening by severe plastic deformation and hardening by annealing of aluminum–zinc alloy: Significance of elemental and spinodal decompositions. *Mater. Sci. Eng. A* **610**, 17 (2014).
10. N.Q. Chinh, T. Csanádi, T. Györi, R.Z. Valiev, B.B. Straumal, M. Kawasaki, and T.G. Langdon: Strain rate sensitivity studies in an ultrafine-grained Al-30 wt.% Zn alloy using micro- and nanoindentation. *Mat. Sci. Eng. A* **543**, 117 (2012).
11. M.V. Borodachenkova, F. Barlat, W. Wen, A. Bastos, and J.J. Gracio: A microstructure-based model for describing the material properties of Al–Zn alloys during high pressure torsion. *Int. J. Plast.* **68**, 150 (2015).
12. N.Q. Chinh, P. Jenei, J. Gubicza, E.V. Bobruk, and R.Z. Valiev: Influence of Zn content on the microstructure and mechanical performance of ultrafine-grained Al–Zn alloys processed by high-pressure torsion. *Mater. Lett.* **186**, 334 (2017).
13. M. Jin, A.M. Minor, E.A. Stach, and J.W. Morris Jr.: Direct observation of deformation-induced grain growth during the nanoindentation of ultrafine-grained Al at room temperature. *Acta Mater.* **52**, 5381 (2004).
14. W. Tillmann, B. Klusemann, J. Nebel, and B. Svendsen: Analysis of the mechanical properties of an arc-sprayed WC–FeCSiMn coating: nanoindentation and simulation. *J. Therm. Spray Technol.* **20**, 328 (2011).
15. E.G. Berasategui and T.F. Page: The contact response of thin SiC-coated silicon systems-characterisation by nanoindentation. *Surf. Coat. Technol.* **163–164**, 491 (2003).
16. G.M. Pharr, W.C. Oliver, and D.R. Clarke: Hysteresis and discontinuity in the indentation load-displacement behavior of silicon. *Scripta Metall.* **23**, 1949 (1989).
17. C.A. Schuh and T.G. Nieh: A nanoindentation study of serrated flow in bulk metallic glasses. *Acta Mater.* **51**, 87 (2003).
18. I.-C. Choi, Y.-J. Kim, B. Ahn, M. Kawasaki, T.G. Langdon, and J.-I. Jang: Evolution of plasticity, strain-rate sensitivity and the underlying deformation mechanism in Zn–22% Al during high-pressure torsion. *Scripta Mater.* **75**, 102 (2014).
19. Y. Liu, J. Hay, H. Wang, and X. Zhang: A new method for reliable determination of strain-rate sensitivity of low-dimensional metallic materials by using nanoindentation. *Scripta Mater.* **77**, 5 (2014).
20. V. Maier, K. Durst, J. Mueller, B. Backes, H.W. Höppel, and M. Göken: Nanoindentation strain-rate jump tests for determining the local strain-rate sensitivity in nanocrystalline Ni and ultrafine-grained Al. *J. Mater. Res.* **26**, 1421 (2011).
21. N.Q. Chinh and P. Szommer: Mathematical description of indentation creep and its application for the determination of strain rate sensitivity. *Mater. Sci. Eng. A* **611**, 333 (2014).
22. K. Durst and V. Maier: Dynamic nanoindentation testing for studying thermally activated processes from single to nanocrystalline metals. *Curr. Opin. Solid State Mater. Sci.* **19**, 340 (2015).
23. B. Merle, V. Maier-Kiener, and G.M. Pharr: Influence of modulus-to-hardness ratio and harmonic parameters on continuous stiffness measurement during nanoindentation. *Acta Mater.* **134**, 167 (2017).
24. J. Hay, P. Agee, and E. Herbert: Continuous stiffness measurement during instrumented indentation testing. *Exp. Technol.* **34**, 86 (2010).
25. A.C. Fischer-Crips: Handbook, “IBIS Uncovered”, Fischer-Crips Laboratories Pty Ltd., P.O. Box 9, Forestville NSW 2087 Australia. (2011).
26. E.G. Herbert, W.C. Oliver, and G.M. Pharr: Nanoindentation and the dynamic characterization of viscoelastic solids. *J. Phys. D: Appl. Phys.* **41**, 074021 (2008).
27. D.A. Woodford: Strain rate sensitivity as a measure of ductility. *Trans. ASM* **62**, 291 (1969).
28. N.Q. Chinh, T. Csanádi, J. Gubicza, R.Z. Valiev, B.B. Straumal, and T.G. Langdon: The effect of grain-boundary sliding and strain rate sensitivity on the ductility of ultrafine-grained materials. *Mater. Sci. Forum* **667–669**, 677 (2011).